Atmospheric Environment xxx (2012) 1–13

Contents lists available at SciVerse ScienceDirect

Atmospheric Environment

journal homepage: www.elsevier.com/locate/atmosenv

Submicron organic aerosol in Tijuana, Mexico, from local and Southern California sources during the CalMex campaign

S. Takahama [a], A. Johnson [a], J. Guzman Morales [a], L.M. Russell [a,*], R. Duran [b], G. Rodriguez [b], J. Zheng [c], R. Zhang [c], D. Toom-Sauntry [d], W.R. Leaitch [d]

[a] Scripps Institution of Oceanography, University of California San Diego, La Jolla, CA 92093-0221, USA
[b] Universidad de Autnoma de Baja California, Tijuana, Mexico
[c] Texas A&M University, College Station, TX, USA
[d] Science and Technology Branch, Environment Canada, Toronto, ON, Canada

HIGHLIGHTS

- Submicron OM composition was measured by FTIR, ACSM, and STXM during CalMex.
- The average OM concentration was 3.3 μg m^{-3} in Tijuana.
- Vehicular sources contributed approximately 40% to the submicron OM.
- OM measured in Tijuana was highly oxygenated (average O/C = 0.6).
- The Southern California Air Basin was a large source of oxygenated OM in Tijuana.

ARTICLE INFO

Article history:
Received 30 October 2011
Received in revised form
18 July 2012
Accepted 19 July 2012

Keywords:
Organic aerosol
Air pollution
FTIR
ACSM
STXM
NEXAFS
Border region

ABSTRACT

The CalMex campaign was conducted from May 15 to June 30 of 2010 to study the properties and sources of air pollution in Tijuana, Mexico. In this study, submicron organic aerosol mass (OM) composition measured by Fourier Transform Infrared Spectroscopy (FTIR), Aerosol Chemical Speciation Monitor (ACSM), and X-ray spectromicroscopy are combined with statistical analysis and measurements of other atmospheric constituents. The average (±one standard deviation) OM concentration was 3.3 ± 1.7 μg m^{-3}. A large source of submicron aerosol mass at this location was determined to be vehicular sources, which contributed approximately 40% to the submicron OM; largely during weekday mornings. The O/C ratio estimated from ACSM measurements was 0.64 ± 0.19; diurnal variations in this value and the more oxygenated fraction of OM as determined from Positive Matrix Factorization and classification analyses suggest the high degree of oxygenation originates from aged OM, rather than locally-produced secondary organic aerosol. A large contribution of this oxygenated aerosol to Tijuana from various source classes was observed; some fraction of this aerosol mass may be associated with non-refractory components, such as dust or BC. Backtrajectory simulations using the HYSPLIT model suggest that the mean wind vector consistently originated from the northwest region, over the Pacific Ocean and near the Southern California coast, which suggests that the origin of much of the oxygenated organic aerosol observed in Tijuana (as much as 60% of OM) may have been the Southern California Air Basin. The marine aerosol contribution to OM during the period was on average 23 ± 24%, though its contribution varied over synoptic rather than diurnal timescales. BB aerosol contributed 20 ± 20% of the OM during the campaign period, with notable BB events occurring during several weekend evenings.

1. Introduction

California and Baja California share a common air basin along the ~200 km border, with sister city pairs of Tijuana–San Diego and Mexicali–Calexico accounting for the highest observed ozone and aerosol concentrations in the urban areas of the border region (Border, 2012). These cities are linked through international commerce that is expected to contribute to increased atmospheric burdens of particulate matter (PM) and gases; rising trends in urbanization suggest that a larger share of the population will be adversely affected by these air pollutants. To study the implications

* Corresponding author.
E-mail addresses: lmrussell@ucsd.ed, lmrussell@ucsd.edu (L.M. Russell).

1352-2310/$ – see front matter © 2012 Elsevier Ltd. All rights reserved.
http://dx.doi.org/10.1016/j.atmosenv.2012.07.057

of current air quality relevant for climate and policy analysis, the CalMex campaign was conducted in Tijuana, Mexico, from May 15 to June 30, 2010, in conjunction with the CalNex campaign that focused on similar issues north of this border.

Atmospheric PM is a mixture of many components, often containing some combination of nitrate, sulfate, ammonium, crustal elements, sea salt, black carbon, and organic molecules (Seinfeld and Pandis, 2006). Of this airborne PM, the number of molecules comprising the organic aerosol fraction are numerous (Hamilton et al., 2004) and undercharacterized (Kanakidou et al., 2005). Our lack of knowledge regarding the constituents and characteristics of this fraction imparts large uncertainties in prediction of aerosol lifetimes (and thus atmospheric concentrations) and climate impacts incurred through aerosol interactions with solar radiation and water vapor. Higher ambient PM mass concentrations have been associated with increased mortality and morbidity (Dockery et al., 1993), posing a risk from a public health perspective.

In this study, we report characterization of the major source classes of organic aerosol to Tijuana and determine the significance of local and transported regional PM to the air quality at this site. We use several analytical methods to characterize the organic aerosol, including FTIR (organic functional groups) and ACSM (non-refractory molecular mass fragments). These measurements are combined with mathematical techniques, additional measurements, and backtrajectory analyses, which have effectively been used for source identification and apportionment for OM in previous campaigns (e.g., Russell et al., 2009; Liu et al., 2009; Hawkins and Russell, 2010; Schwartz et al., 2010; Frossard et al., 2011; Takahama et al., 2011).

2. Methods

2.1. Sampling site

The measurements (Table S1) were collected in a trailer installation at Parque Morelos, located in the Southeast region of Tijuana (32.52°, −117.037°, 6 m.a.s.l.). The park is an ecological reserve and recreational park surrounded by roadways, shopping centers, and residential neighborhoods, and situated less than 15 km from the San Ysidro border station.

2.2. Organic functional group composition

Atmospheric particles were sampled on Teflon filters [with filter changes at approximately 06h00, 14h00, and 18h00 Pacific Standard Time (PST) daily] and analyzed by Fourier Transform Infrared Spectroscopy (FTIR) for organic functional group (OFG) composition. The filters were analyzed immediately after removal from storage for FTIR analysis. Infrared sample spectra were obtained with a Tensor 27 spectrometer (Bruker, Billerica, MA), baselined, and fitted with peaks to identify OFG using the method described by Russell et al. (2009). Using this method, FTIR spectroscopy provides OFG concentrations, including alkane, carboxylic acid, organic hydroxyl, primary amine, and carbonyl groups through chemical bond-based measurements in atmospheric particles collected on a substrate (Russell et al., 2009). Alkene, aromatic, and organosulfate groups were below detection limit for all samples. Our discussion of OM will therefore neglect these compounds; their contribution to the actual OM is estimated to be between 2 and 5%. Ketone group contributions are estimated from a comparison of moles of carboxylic COH and total carbonyl quantified; non-acid carbonyl contributions (including aldehydes and ketones) are determined by the moles of carbonyl present in excess of quantified moles of carboxylic COH. The non-acid carbonyl is determined to be ketonic rather than aldehyde carbonyl, as absorption bands between 2700 cm^{-1} and 2860 cm^{-1} indicative of aldehydic hydrogen were not observed in the sample spectra. The quantified non-acid carbonyl will therefore be referred to as ketones in this manuscript. The uncertainty and detection limit of ketones are therefore estimated through a contribution of the estimated carboxylic COH and total carbonyl (Russell et al., 2009). Estimation of mass is based on the analysis by Russell (2003), where moles of measured bonds are converted to the moles of comprising atoms, and values of OM are calculated from the sum of moles of atoms multiplied by their respective molecular weights. Using this approach, the uncertainty in OM has been calculated to be on the order of 21% (Russell, 2003).

2.3. Non-refractory organic and inorganic mass concentrations

The Aerodyne Aerosol Chemical Speciation Monitor (ACSM; Ng et al., 2011b) with a Pfeiffer Prisma quadrapole was used to scan over 150 mass/charge (m/z) units at a rate of 0.5 m/z per second. The ACSM is similar to the Aerodyne Aerosol Mass Spectrometer (AMS; Jayne et al., 2000) with the primary differences being the absence of a particle time-of-flight measurement and reduced sensitivity in the ion signals. Differences in measured signal between 6 to 12 aerosol-containing and aerosol-free air (using filter mode) are averaged over 15–30-min intervals for each measurement. The absolute and relative ionization efficiencies of nitrate and ammonium, respectively, are calibrated with nearly monodisperse particles (10:1 sheath to sample flowrate on a TSI, Inc. 3071 differential mobility analyzer and counted with a 3010 Condensation Particle Counter), and the relative ionization efficiencies for sulfate and organics are based on the AMS (Ng et al., 2011b). A diffuse naphthalene source is nominally used as an internal standard to normalize the measurements with respect to temperature and pressure; this source was depleted toward the end of the campaign so the closed signal of the m/z 32 associated with the airbeam is used for the corrections instead. Software provided by Aerodyne, Inc. is used to process the measurements to obtain concentrations of sulfate, nitrate, ammonium, chloride, and total organic aerosol, and organic mass fragment spectra. Further details are discussed by Ng et al. (2011b). A correction factor of 0.3 is used to scale the final ACSM concentrations such that the reported OM agrees with the FTIR; corrections of this type are anticipated to account for non-unit transmission and particle collection efficiencies associated with the ACSM (Ng et al., 2011b). The scaling is linear (no intercept) and therefore does not affect the conclusions regarding OM composition presented in this manuscript, which are based primarily on relative fractions and temporal variations of ACSM-measured components of OM. This correction factor has also been applied to non-refractory PM_1 (NR-PM_1) and its components hereafter reported in this manuscript. Following conventions adopted by the AMS community (e.g., Ng et al., 2010, 2011b), the mass fragment concentrations are reported either in C_x [the OM-equivalent mass concentration of mass fragment (m/z) x], f_x [the OM-normalized mass concentration of mass fragment (m/z) x], or as integrated values of SO_4, NO_3, NH_4, Cl, and OM (also commonly referred to as “OA” or “Org”).

2.4. Dimension reduction methods

Positive Matrix Factorization (PMF; Paatero and Tapper, 1994) is commonly used for the analysis of environmental measurements, and more specifically, for the inversion of observed infrared and mass fragment spectra into a set of constituent components. Given a column matrix of row vectors (i.e., the sample spectra), $\boldsymbol{X}$, the forward model is expressed as $\boldsymbol{X} = \boldsymbol{GF} + \boldsymbol{E}$. $\boldsymbol{G}$ and $\boldsymbol{F}$ are matrices comprising component strengths and profiles, respectively; $\boldsymbol{E}$ is the

Please cite this article in press as: Takahama, S., et al., Submicron organic aerosol in Tijuana, Mexico, from local and Southern California sources during the CalMex campaign, Atmospheric Environment (2012), http://dx.doi.org/10.1016/j.atmosenv.2012.07.057

residual matrix. The Q (or χ^2) value to be minimized is defined by the canonical objective function $Q = \sum\sum e_{ij}^2/s_{ij}^2$, where e_{ij} are the residuals (elements of $\boldsymbol{E}$) and s_{ij} define the weighting for the fit. Details are described in Section S1.1.

Conceptually, PMF analysis permits determination of the relative proportion of each component in a sample mixture, provided that the inverse problem is well-constrained. When a possible set of components are hypothesized a priori, classification of the mixture data allows us to determine the components most similar to each reported observation according to a prescribed algorithm, and provides an additional tool by which we can evaluate among the possible solutions obtained through PMF decomposition. For this purpose, two supervised learning methods – k-nearest neighbor (k-nn) and linear discriminant analysis (LDA) – are also used for the classification of ACSM spectra against a set of training spectra. The training spectra consist of two subcategories of oxygenated organic aerosol (OOA): OOA-1, OOA-2; hydrocarbon-like organic aerosol (HOA); and biomass burning organic aerosol (BBOA), which are PMF components archived from various AMS studies (Ulbrich et al., 2009, 2012). Further details are included in Sections 3 and S1.3; results are summarized in Table S2.

2.5. Elemental analysis

Samples used for FTIR analysis were also used for measurement of elemental composition by X-ray fluorescence (XRF). Ninety of the same filter samples used for FTIR were sent to Chester LabNet (Tigard, Oregon) for mass quantification of Na and heavier elements (EPA Protocol 6).

2.6. Black carbon number concentrations

An 8-channel Single Particle Soot Photometer (SP2; Droplet Measurement Technologies, Inc.) measures individual particle responses upon interaction with a Nd:YAG laser (1064 nm). Particles containing black carbon (BC) absorb the energy and thermally irradiate as they vaporize at approximately 4000 K. The emitted thermal radiation (at visible wavelengths) is detected with red and blue sensitive photomultipliers. A calibration curve was generated by SP2 response to particles atomized from Aquadag in aqueous solution and size selecting them by using a TSI Electrostatic Classifier. Thresholds for event detection for high-gain and low-gain channels were set to 2500 and 100 counts, respectively, based on analysis of signal count histograms. The lower detection limit has been reported to be on the order of 0.7 fg, or 90 nm in mass-equivalent diameter (Schwarz et al., 2010).

2.7. X-ray spectromicroscopy analysis

Scanning Transmission X-Ray Microscopy with Near-Edge X-Ray Absorption Fine Structure (STXM-NEXAFS; Stöhr, 1992) with processing algorithms described by Takahama et al. (2010) was also used to examine single particle morphology and composition for a limited number of particles. With this method, X-rays generated at the Advanced Light Source at Lawrence Berkeley National Laboratories (Beamline 5.3.2) are used to probe the electronic structure of individual particles at a spatial resolution of approximately 30 nm. Collectively, 39 particles were analyzed from the campaign period.

2.8. Proton-Transfer-reaction mass spectrometry

A Proton-Transfer-Reaction Mass Spectrometer (PTR-MS) was used to measure the concentrations of volatile organic compounds (VOCs) by facilitating proton-transfer reactions in a drift-tube reaction chamber between gas-phase species and H_3O^+ ions generated by an ion source (Lindinger et al., 1998; Warneke et al., 2003). Gas-phase concentrations of benzene, toluene, and C_8 and C_9 aromatics measured by this instrument (Zhao and Zhang, 2004; Zhao et al., 2005; Fortner et al., 2009) are used for this study.

2.9. Backtrajectory analysis

Airmass back and forward trajectories were obtained from the HYbrid Single Particle Lagrangian Integrated Trajectory Model (NOAA HYSPLIT; Draxler and Rolph, 2010). Three-day back-trajectories were calculated every hour for the duration of the campaign at heights of 10, 100, and 500 m above ground level to consider the uncertainty of trajectories due to initial conditions. Mixing heights calculated by the HYSPLIT model were also extracted from the trajectory simulations.

3. Results and discussion

The non-refractory submicron aerosol composition measured by ACSM during the campaign was 5.8 ± 5.1 μg m^{-3} on average (±one standard deviation shown), with contributions from sulfate (14 ± 7%), nitrate (17 ± 10%), ammonium (12 ± 7%), chloride (3 ± 3%), and organic aerosol (53 ± 14%) (Fig. 1). Trends in diurnal variations indicated organic aerosol, nitrate, and NR-PM_1 in general peaked during morning hours (06h00–10h00 PST; Fig. 2), with similar traffic activity observed during both weekdays and weekends. Mixing layer heights estimated by HYSPLIT indicate that the boundary layer begins to rise around 06h00 PST, so this increase in concentration is observed in spite of a rising boundary layer (which has a diluting effect). The following sections will describe the organic aerosol fraction in more detail and discuss inferred source classes and regions.

3.1. Submicron organic aerosol composition

3.1.1. FTIR analysis

The organic aerosol fraction as measured by FTIR during the campaign was 3.3 ± 1.7 μg m^{-3} on average, with contributions from alkane (44 ± 9%), organic acid (26 ± 7%), organic hydroxyl (22 ± 13%), primary amine (5 ± 2%), ketone (3 ± 5%), and organonitrate (<1%) groups (Fig. 3). The average organic aerosol composition was similar to that measured during previous campaigns in urban areas: Houston (Texas GoMACCS), Mexico City (MILAGRO), and Atlantis (CalNex) off the coast Southern California, while different from those measured in more remote areas (Fig. 4). These campaigns were conducted during different times and months (with the exception of CalNex Atlantis, which was measured concurrently), but the similarity of measured composition to Houston and Mexico City may reflect the large contribution from anthropogenic combustion sources which are the major source classes to these locations. As discussed in Section 3.3, the similarity of composition to Atlantis with the exception of ketone groups from burning episodes may also be attributed to common sources or airmasses.

3.1.2. ACSM analysis

The organic mass fragments from ACSM suggest a highly oxygenated aerosol, with an average O/C value of 0.64 ± 0.19 estimated for the campaign using the f_{44} parameterization by Aiken et al. (2008). This value is relatively high with respect to O/C ratios compiled by Aiken et al. (2008) for urban locations, and would be more closely associated with values observed in urban outflows. There is a possibility that a bias is introduced in estimating O/C from a parameterization developed for the AMS in

Please cite this article in press as: Takahama, S., et al., Submicron organic aerosol in Tijuana, Mexico, from local and Southern California sources during the CalMex campaign, Atmospheric Environment (2012), http://dx.doi.org/10.1016/j.atmosenv.2012.07.057

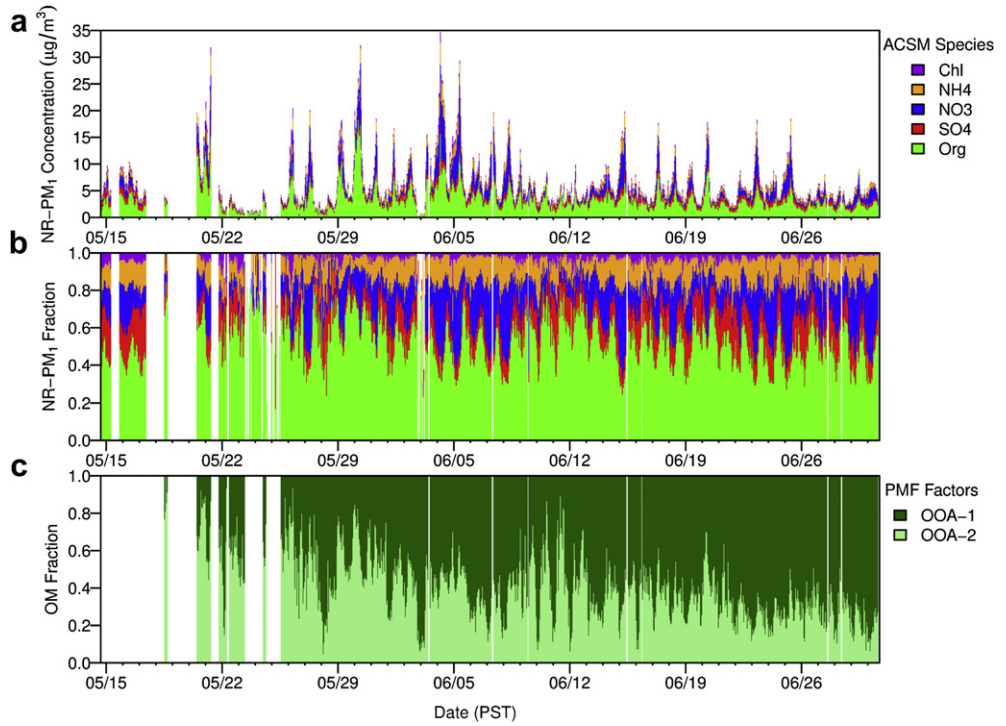

Fig. 1. Time series of (a) NR-PM_1 concentrations, (b) NR-PM_1 component fractions (normalized by sum of NR-PM_1) (c) OM fractions of PMF components.

Mexico City to the ACSM in Tijuana. Results reported by Ng et al. (2011b) suggest that AMS and ACSM spectra interpretation are comparable at Queens, NY, but the existence of some bias due to measurement of aerosol populations at a new geographical region with different size and composition cannot be ruled out. The average O/C measured by FTIR is 0.52 ± 0.16 (Fig. 5a), though this average and much of its variation are due to large contribution from the marine fraction of OM. A direct O/C comparison with ACSM indicates a mild correlation with non-hydroxyl O/C (r = 0.46; Fig. 5b); some correlation between these two values is expected as the mass fragment on which O/C is parameterized for the ACSM is the m/z 44 (COO^+) fragment. This fragment is assumed to be

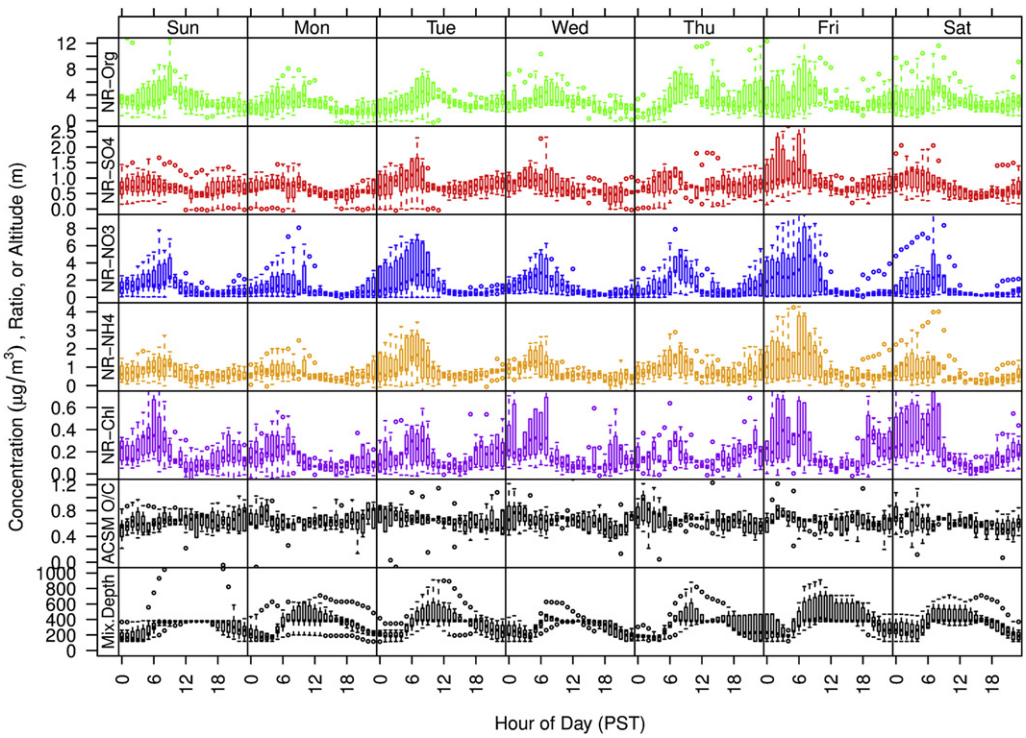

Fig. 2. Diurnal variations by day of week for non-refractory components, O/C ratio estimated with ACSM, and mixing heights (Mix.Depth) retrieved from NOAA's HYSPLIT model.

Please cite this article in press as: Takahama, S., et al., Submicron organic aerosol in Tijuana, Mexico, from local and Southern California sources during the CalMex campaign, Atmospheric Environment (2012), http://dx.doi.org/10.1016/j.atmosenv.2012.07.057

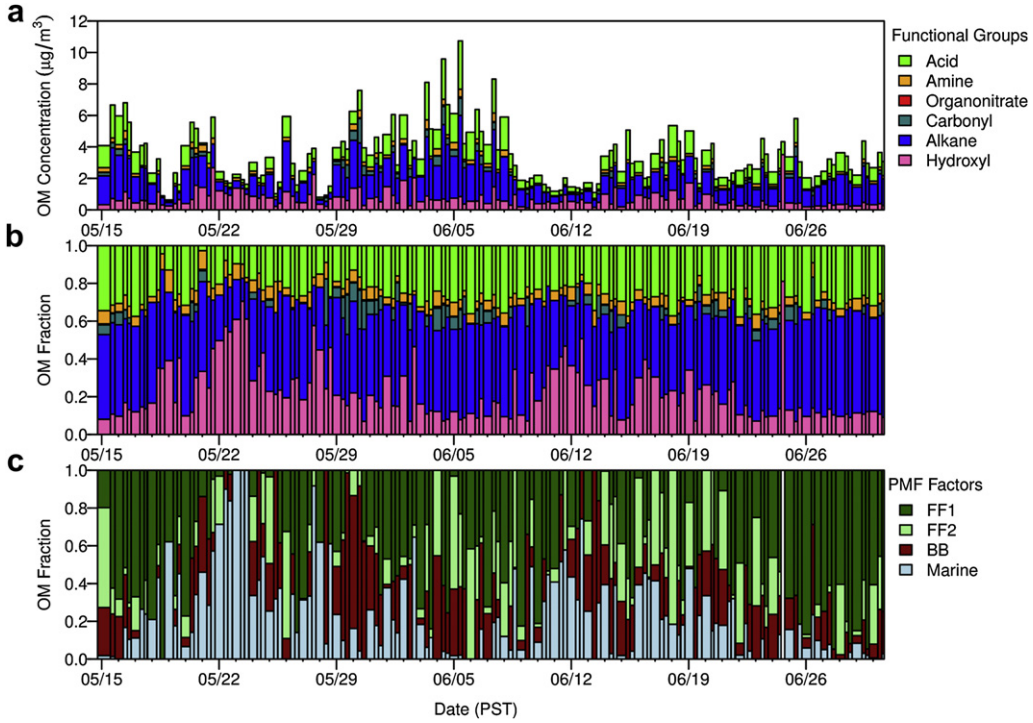

Fig. 3. Time series of (a) OFG concentrations, (b) OFG concentrations normalized by total OM, and (c) OM fraction of PMF components.

produced largely through the fragmentation of carboxylic acid groups (Russell et al., 2010; Ng et al., 2011b) rather than hydroxyl groups in alcohol or phenol compounds. Without O/C contributions from hydroxyl groups, the estimated FTIR O/C is approximately 0.3 ± 0.1, which is low but closer to what has been reported for urban areas by AMS observations (Aiken et al., 2008). As discussed in Section 3.2, the marine fraction of OM as determined from PMF analysis has an O/C ratio of ~1, but the rest of the contributing components range between 0.4 and 0.6, with the most predominant component (fossil-fuel combustion) having an O/C of about 0.4 (Fig. 6). The magnitude of O/C overall is considerably lower for FTIR than estimated for the ACSM (especially when hydroxyl functional groups are excluded); this bias has also been reported in a previous FTIR-AMS comparison for the Texas GoMACCS campaign (Russell et al., 2009), and may reflect the differences in the analytical techniques and estimation methods used by spectroscopic and mass fragment analysis approaches to organic aerosol measurement. The ACSM O/C ratio most notably does not appear to show a strong diurnal variation (Fig. 1) as observed in Mexico City, where larger O/C values were observed in the afternoon periods corresponding to formation of SOA (Aiken et al., 2008; de Gouw et al., 2009).

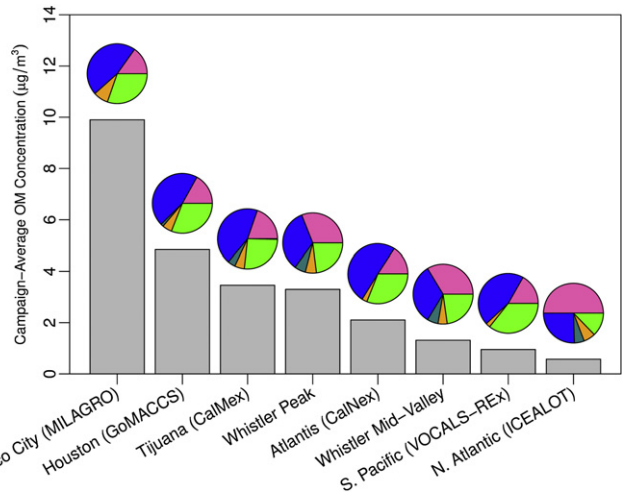

Fig. 4. Average OM concentrations (bar plots) and fractional contributions of OFG (pies) for various campaigns for which comparable FTIR measurements are available. Colors indicate contributions of individual functional groups to OM, and are defined in Fig. 3. Analysis for MILAGRO by Liu et al. (2009), GoMACCS by Russell et al. (2009), Whistler peak by Takahama and Russell (2011), Whistler Mid-Valley by Schwartz et al. (2010), VOCALS-REx by Hawkins and Russell (2010), and ICEALOT by Frossard et al. (2011). (For interpretation of the references to color in this figure legend, the reader is referred to the web version of this article.)

If we examine the chemical composition in f_{43}–f_{44}–f_{57}–f_{60} space (Fig. 7; based on precedent by Ng et al., 2010; Cubison et al., 2011; among others), we expect that the measurements in Tijuana most frequently fall within bounds delineated by oxygenated organic aerosol (OOA), more oxygenated OOA (OOA-1), and less oxygenated OOA (OOA-2). Though OOA is conceptually a superset of OOA-1 and OOA-2, the labels reflect categorizations provided by individual researchers in separate campaigns. This observation is more formally supported by classification analyses using LDA and *k*-nn in this domain (Fig. S2). These supervised learning methods suggest that most observations (~90%) would be classified as some type of OOA, with approximate ensemble compositions around 69–77% OOA-1 and 20–26% OOA-2 (Fig. 8a). The ensemble analysis of classified ACSM mass spectra indicate that the OOA-2 is more frequently observed during morning (06h00–09h00 PST) and evening (17h00–20h00 PST) hours, consistent with the picture that a higher fraction of hydrocarbons are present in organic aerosols associated with vehicle-related emissions. The fraction of the more oxygenated OOA-1 is higher during late evening and early morning hours, which may reflect the varying contribution of OOA-2 to the total OM in addition to the effect of continued aging of organic aerosol after hydrocarbon emissions from anthropogenic activity have been reduced.

Please cite this article in press as: Takahama, S., et al., Submicron organic aerosol in Tijuana, Mexico, from local and Southern California sources during the CalMex campaign, Atmospheric Environment (2012), http://dx.doi.org/10.1016/j.atmosenv.2012.07.057

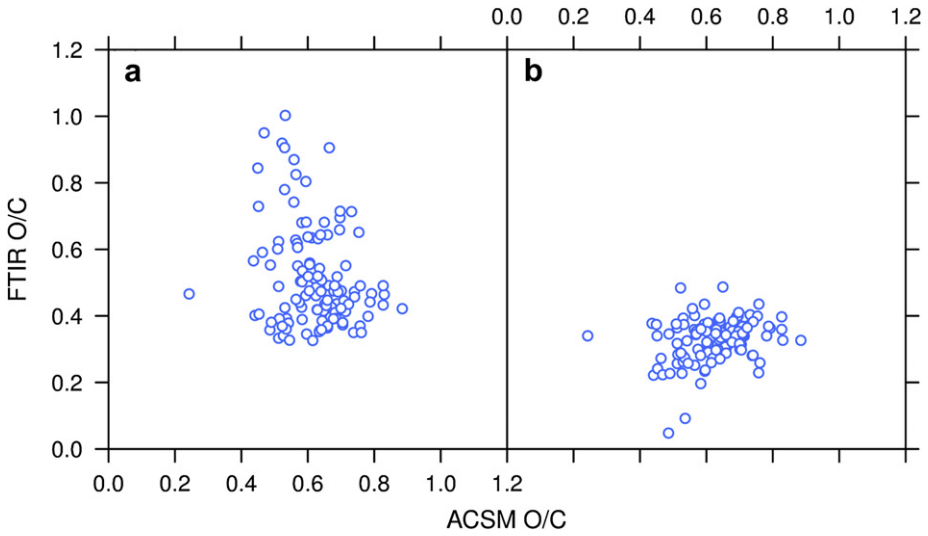

Fig. 5. O/C estimates for ACSM and (a) FTIR, and (b) FTIR excluding hydroxyl functional-group contributions to O/C values.

3.2. Source classes of PM_1 organic aerosol at Parque Morelos

3.2.1. PMF analysis of FTIR spectra

A four-factor solution was selected from PMF decomposition of FTIR spectra matrix (Fig. 9). The first factor was correlated with elemental tracers commonly associated with anthropogenic combustion (S and V; Fig. 10) and its spectra profile is similar to that of fossil fuel combustion from previous campaigns. A second factor was also correlated with S (Fig. 10) but was more oxygenated with an O/C of ~0.6 (as opposed to 0.4 for the first factor; Fig. 6). These factors will be referred to as FF1 and FF2 following the convention used by Russell et al. (2011) for fossil-fuel combustion-derived components. Alkane and carboxylic acid functional groups were the major components of these two types of fossil fuel combustion classes; this has been attributed to emission of hydrocarbons and oxidative processes in the atmosphere producing organic acids. Another factor is correlated with elemental tracers for marine aerosol (Na and Cl, presumably from sea salt; Fig. 10) and its spectral profile is similar to that of marine aerosol from previous campaigns and laboratory standards of saccharides Russell et al. (2010, 2011). This marine factor accounted for 45 ± 32% of the hydroxyl functional group mass concentrations measured during the campaign. The last factor was correlated with K (Fig. 10), an elemental tracer for burning, and will therefore be referred to as biomass burning (BB). This factor was also correlated with elements not commonly associated with burning of biomass such as S and V (Fig. 10), so this component may also incorporate burning events from incineration, fuel-burning, or other anthropogenic activity. This factor accounted for all of the detectable ketonic carbonyl measured during the campaign. Elevated concentrations of ketones have been observed in burning samples in San Diego (Hawkins and Russell, 2010) and Whistler Peak (Takahama et al., 2011). The relative contribution of primary amine groups to the OFG concentration was not substantially higher during the BB periods as observed aboard the Ron Brown during the ICARTT campaign (Bahadur et al., 2010) or at Whistler Peak (Takahama et al., 2011). Elevated amine concentrations have been reported in BB aerosol elsewhere (e.g., Laskin et al., 2009), but variations in their contributions to the BB aerosol fraction may indicate differences in emissions or gas-particle conversions (Ge et al., 2011). Regions of the spectra (~860 cm^{-1}) associated with organonitrate absorption (Garnes and Allen, 2002; Day et al., 2010) were not included in the PMF decomposition, but a posteriori correlation of organonitrate mass concentrations with BB OM ($r = 0.8$) indicates the presence of organic nitrate compounds in the aerosol phase during BB events. While an elevation in organonitrate aerosol concentrations was detected, the overall concentration of organonitrate compounds in the condensed phase remained less than one percent of the OM mass during these periods.

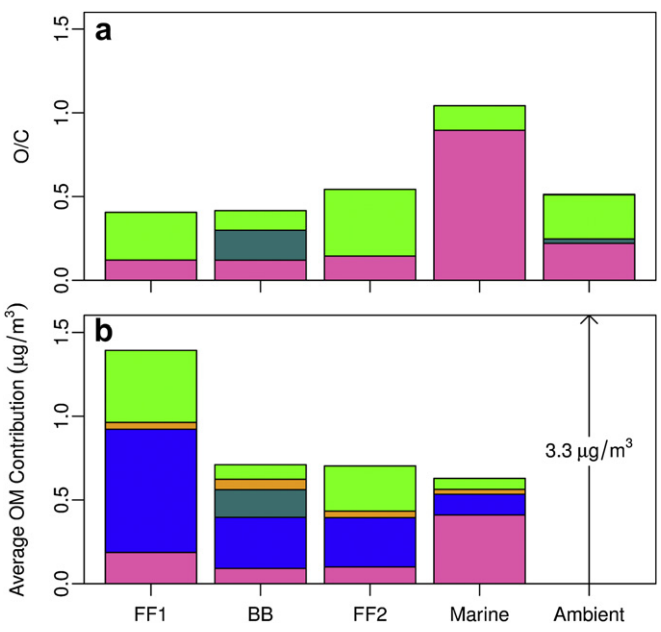

Fig. 6. Estimates of (a) O/C ratios and (b) average contributions to OM during the campaign for FTIR PMF components. Colors indicate contributions of individual functional groups to O/C or OM, and are defined in Fig. 3. (For interpretation of the references to color in this figure legend, the reader is referred to the web version of this article.)

3.2.2. PMF analysis of ACSM spectra

While HOA and various types of OOA are commonly found in other locations (e.g., Zhang et al., 2005, 2007; Jimenez et al., 2009), the degree of oxygenation as indicated by the ACSM mass fragment measurements and classification analyses discussed in Section 3.1

Please cite this article in press as: Takahama, S., et al., Submicron organic aerosol in Tijuana, Mexico, from local and Southern California sources during the CalMex campaign, Atmospheric Environment (2012), http://dx.doi.org/10.1016/j.atmosenv.2012.07.057

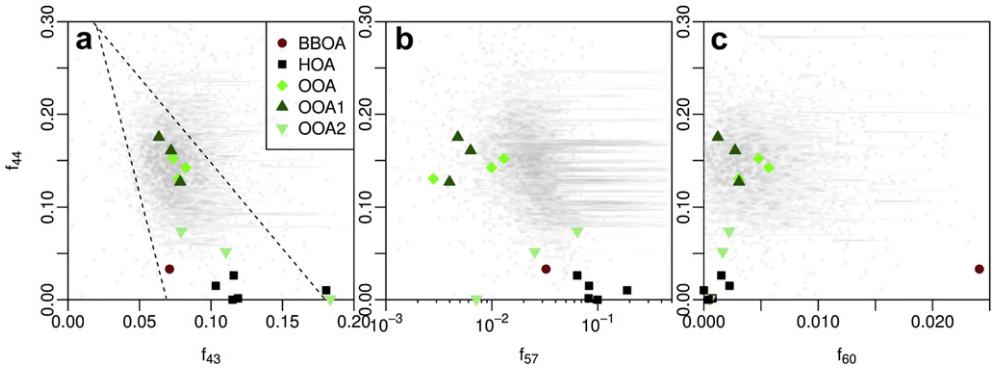

Fig. 7. Normalized mass fragment concentrations (Section 2) projected into f_{43}–f_{44}–f_{57}–f_{60} space. Gray points indicate Tijuana ambient measurements. Colored symbols represent PMF components extracted from previous campaigns in other locations (provided through AMS Spectral Database; Ulbrich et al., 2009, 2012). (For interpretation of the references to color in this figure legend, the reader is referred to the web version of this article.)

suggest that an all-OOA PMF solution is a plausible interpretation of the ACSM spectra for Tijuana during this campaign period (Fig. 11). A possible deconvolution (in the spectral sense) into HOA and OOA can be forced through regression analysis with mass fragment apportionment parameters proposed from previous campaigns (Ng et al., 2011a) (Section S2.1). However, no HOA and OOA solution was found to be feasible within the specification of our PMF analysis (Sections 2 and S1.1). Similarity of selected PMF factor profiles (with O/C ratios of 0.7 and 0.4, respectively) within the composition space of OOA-1 and OOA-2 reported previously (Ng et al., 2010;; with slight differences) argues in favor of adopting these naming conventions for our components. It is perhaps more appropriate to propose that a two-component solution yields a pair of oxygenated and less-oxygenated components along of continuum of oxygenation, as the temporal variations of each component (according to PMF and regression analysis) are approximately the same (Section S2.1). Within this robust finding, we can find a systematic difference in the OM mass apportioned between the two components (Section S1.5), but primarily discuss our interpretation from the perspective of the PMF analysis.

Our selected PMF solution for ACSM spectra suggests that the aerosol mixture composition is approximately 40 ± 19% OOA-2 and 60 ± 19% OOA-1 during the campaign, though the OOA-2 fraction is higher during the earlier period of the campaign when the OM concentrations are higher (r = 0.46; Fig. 1c). Elevated m/z 60 concentrations are observed during BB events, but the frequency of

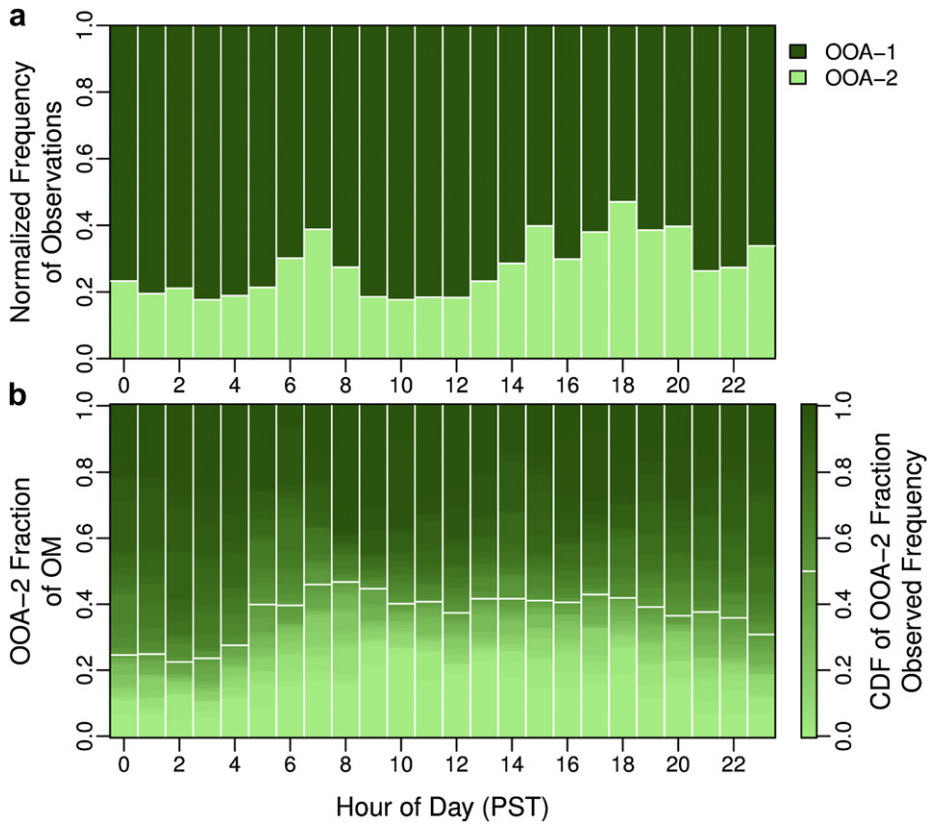

Fig. 8. Ensemble statistics of OOA-1 and OOA-2 contributions to hour of day during the campaign as estimated by (a) LDA and (b) PMF. Color gradient in panel (b) corresponds to cumulative distribution function (CDF) of OOA-2 fraction of OM, with a white line demarcating the location of the median. (For interpretation of the references to color in this figure legend, the reader is referred to the web version of this article.)

Please cite this article in press as: Takahama, S., et al., Submicron organic aerosol in Tijuana, Mexico, from local and Southern California sources during the CalMex campaign, Atmospheric Environment (2012), http://dx.doi.org/10.1016/j.atmosenv.2012.07.057

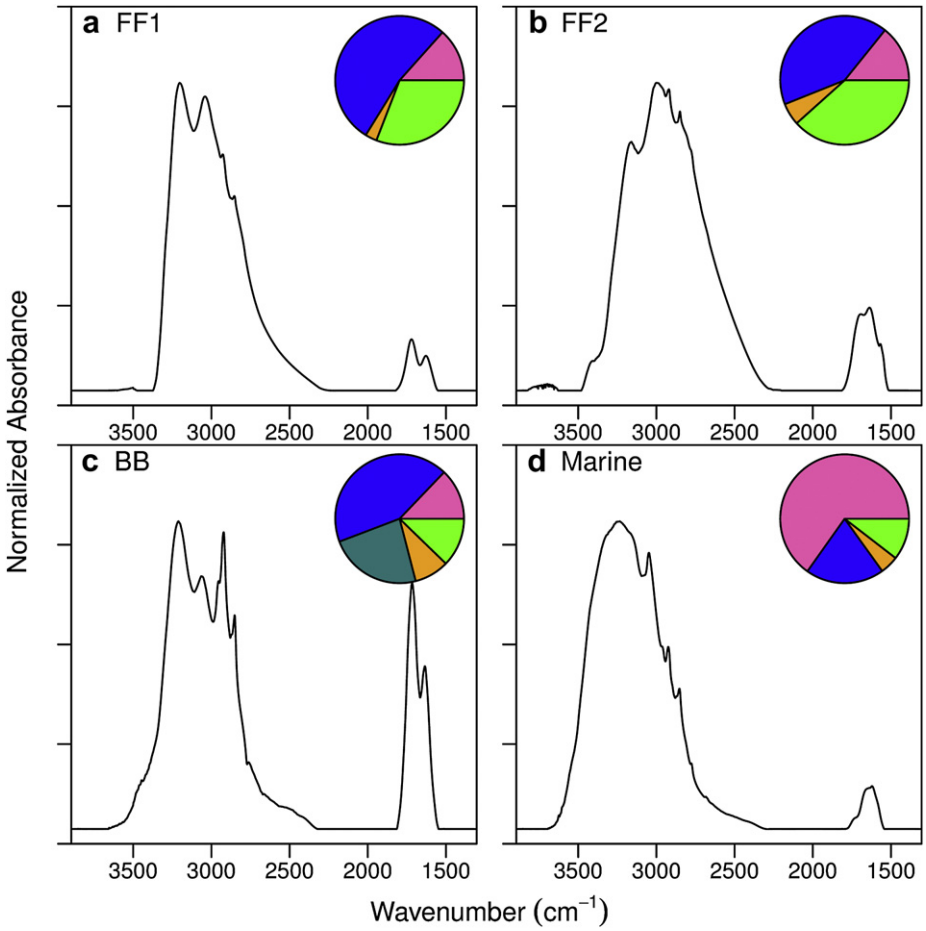

Fig. 9. FTIR PMF factor profile spectra and relative functional group composition. Colors indicate contributions of individual functional groups to OM, and are defined in Fig. 3.

observation and relative magnitudes of contribution are too low for a BB PMF component to be separated from the ACSM mass spectra. Statistics on the ensemble indicate that the OOA-2 fraction is frequently higher during elevated traffic activity periods at 06h00-09h00 (PST) and late afternoon (Fig. 8b) and lower during evening and early morning hours. Several aspects of this diurnal profile are qualitatively consistent with trends indicated by the classification analysis (Fig. 8b). Robust features include the rise of OOA-2 around periods of peak traffic activity and higher fraction of oxygenated aerosol during late evening and early morning hours. An additional

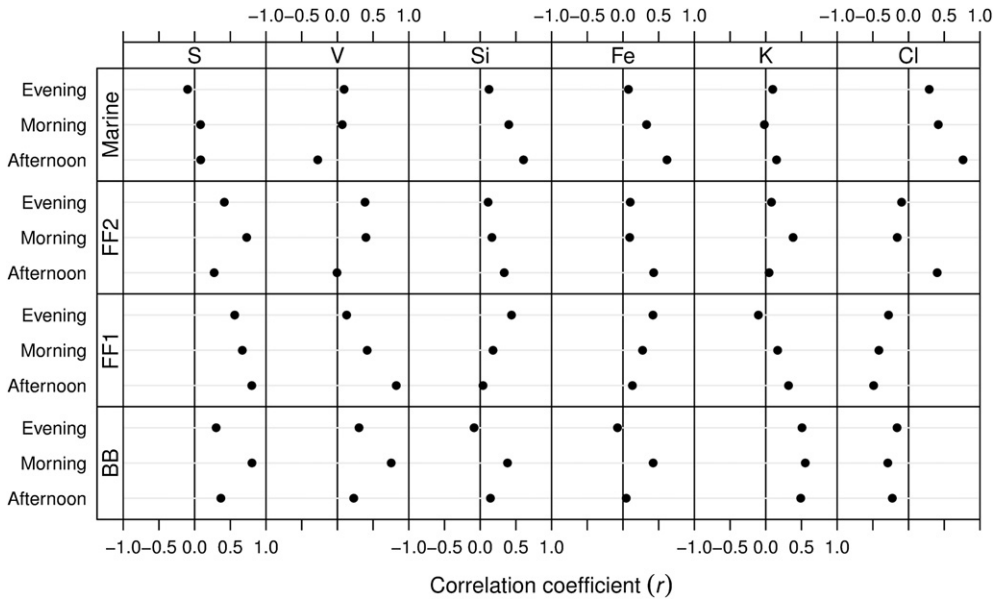

Fig. 10. FTIR PMF factor OM correlations with elements from XRF analysis.

Please cite this article in press as: Takahama, S., et al., Submicron organic aerosol in Tijuana, Mexico, from local and Southern California sources during the CalMex campaign, Atmospheric Environment (2012), http://dx.doi.org/10.1016/j.atmosenv.2012.07.057

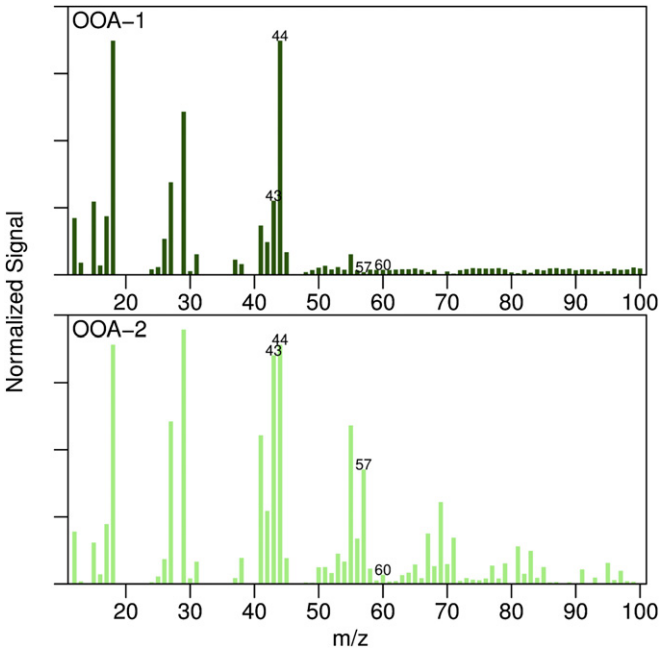

Fig. 11. ACSM PMF factor mass spectra.

regular feature includes small increases of oxygenated aerosol fraction (OOA-1) around 12h00 PST, which is the period of maximum solar intensity and therefore UV-initiated photochemistry. An alternative method of separation in which apportionment is forced into HOA and OOA categories using OM-equivalent concentrations of m/z 44 and m/z 57 mass fragments is discussed in Section S1.5, and supports the diurnal variations captured by this PMF solution (while in this case the less-oxygenated HOA fraction is estimated to be significantly lower). The combined interpretation from these analyses is that the ACSM mass spectra are separable into two components, one of which is less oxygenated than the other. The correlation of factor strengths ($r = 0.77$ for OOA-2 and HOA, and 0.86 for OOA-1 and OOA, respectively) suggests that the less oxygenated component is likely to be associated with primary emissions that are emitted locally (based on the assumption that HOA can be interpreted as POA; e.g., Liggio et al., 2010). The estimate of the primary fraction differs by 28% (of 3.3 μg m^{-3}) depending on which interpretation is selected, but is robust with respect to the temporal trends that are represented by this component (Section S1.5).

3.2.3. Source identification from time-resolved measurements

Examination of time-resolved OM from ACSM with black carbon number concentrations from the SP2 for morning periods indicate that co-emission of OM from traffic combustion sources may be a large contributor to overall OM, as indicated by correlations with m/z 57, and OOA-2 (Fig. 13). The correlations of these components with BC for weekday mornings are milder than for the weekend mornings because there is larger variability in OM concentrations relative to BC, possibly suggesting additional sources during weekday morning periods. In contrast, mild correlations of OM and m/z 57, OOA-2, and additionally m/z 60 with SP2 BC number concentrations (Fig. 13) during several weekend evenings (notably 5/30, 6/13, and 6/20 corresponding to periods between Saturday night and Sunday mornings) suggest that the BB sources are large contributors to OM during these periods. Correlations of BC concentrations with FTIR factors support these statements, with $r = 0.72$ with the BB factor on weekend evenings, and $r = 0.58$ and 0.46 with the FF1 factor on weekday mornings and weekend afternoons, respectively. Examination of diurnal variation in VOC concentrations further support attribution of OOA-2 to vehicular combustion. Concentrations of VOCs traditionally associated with anthropogenic emissions – benzene and heavier (C_8, C_9) aromatic compounds, often associated with diesel exhaust (Jobson et al., 2005) – have correlation of $r = 0.51$–0.53 with OOA-2 within the same hour (Fig. S5).

3.2.4. The nature of BB aerosol at the Parque Morelos site

Hydroxyl functional groups present in levoglucosan and anhydrous sugars reported in fresh BB sources (Fine et al., 2002; Sullivan et al., 2008) are found in small quantities in the FTIR BB factor, while m/z 60 concentrations from ACSM are still correlated ($r = 0.70$) with this component. This observation is consistent with findings by Hawkins and Russell (2010) and Takahama et al. (2011). The BB samples reported in these past studies had been aged over long transport times; given the large number of fires reported in Tijuana during the campaign period and instances of visible smoke at the sampling site, the BB aerosol sampled here are thought to be attributed to more local sources during most periods. The relative fraction of hydroxyl groups is slightly higher in the BB factor observed during the CalMex campaign, and this may reflect differences in age (Hennigan et al., 2010). While the m/z 60 signal did increase during BB events, the OM-normalized f_{60} fraction was not correlated ($|r| < 0.2$) with BB OM or carbonyl functional groups measured by FTIR. Additionally, periods during which f_{60} increased above the background levels of 0.3 ± 0.06% (defined by Cubison et al., 2011) did not correspond to periods of BB in our samples. Our mean and standard deviation for f_{60} values for the campaign were 0.3 ± 0.14% (Fig. 7), and no significant differentiation in this metric between BB and non-BB periods as determined by FTIR was observed. This observation may possibly reflect the presence of additional organic mass in the BB aerosol in Tijuana. Co-occurrence of anthropogenic elements reported by XRF analysis (Fig. 10) suggests that the composition of this BB aerosol may be different from BB aerosol previously reported in the literature. Combined with the observation of increase in total organic aerosol concentration during these BB periods, it is possible that the composition domain is not sufficiently distinguished by f_{60} for the burning events observed in Tijuana during this campaign.

3.2.5. Synthesis and OM apportionment

From the FTIR PMF analysis, we find that the largest contributor to submicron OM to Tijuana during this campaign is FF combustion, comprising 40 ± 28% less oxygenated and 17 ± 19% more oxygenated fractions, with marine and BB components also contributing approximately 20% each (Fig. 6). ACSM mass fragment analysis indicates the presence of very oxygenated aerosol overall (mean O/C of 0.64 ± 0.19), and the more oxygenated of the two ACSM PMF components (OOA-1) is, on average, the larger contributor to the organic aerosol fraction of submicron OM. Its contributions are most frequently highest during evening hours, suggesting nighttime production and/or accumulation under a shallow planetary boundary layer. The less oxygenated OOA (OOA-2) is found to peak most frequently during morning hours, corresponding to traffic activity in Tijuana and consistent with expectations that aerosol containing more hydrocarbon-like molecules would be present during periods influenced by this source category. Because FTIR sampler filter changes occurred each morning at 07h00, the peak loadings from this source (traffic) were sampled on both the evening and morning samples. The relative contributions of OOA-1 and OOA-2 to Tijuana OM largely characterize the degree of aerosol oxygenation from a mixture of source classes, as indicated with correlations with FTIR PMF components (BB, $r = 0.70$, 0.63; FF1,

Please cite this article in press as: Takahama, S., et al., Submicron organic aerosol in Tijuana, Mexico, from local and Southern California sources during the CalMex campaign, Atmospheric Environment (2012), http://dx.doi.org/10.1016/j.atmosenv.2012.07.057

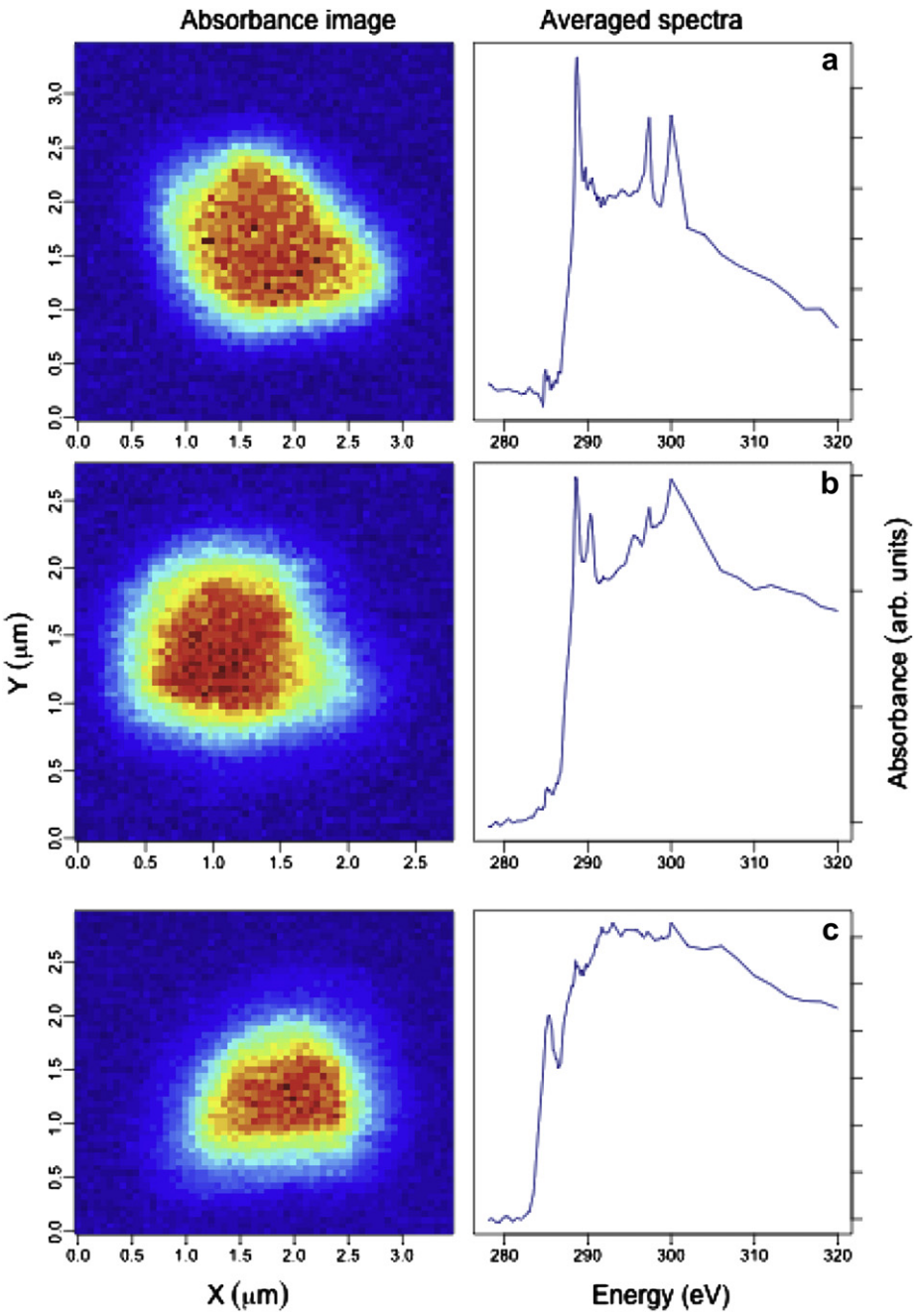

Fig. 12. Example STXM-NEXAFS images and spectra for (a) organic acid-dominated, (b) organic-dust, and (c) organic-black carbon particles.

$r = 0.36, 0.03$; FF2, $r = 0.35, 0.16$ for OOA-1 and OOA-2, respectively). These correlations also suggest that the split by degree of oxygenation for the FTIR FF factors and ACSM OOA factors is relative to the measurement by each instrument and not necessarily universal or absolute, though the coarse time resolution of the FTIR may also have an effect in the resolvability of component contributions (Henry, 2003). As discussed in Section S2.1, approximately 50–60% of the OM associated with FF factors is associated with OOA-1, suggesting an estimate for the anthropogenic contribution from remote sources (Sections 3.3 and S2.1).

There is some evidence that the weak (or lack of) correlation between FTIR FF2 and ACSM PMF factors may be due to the difference in the fraction of OM that is quantified by the two instruments. The stronger correlation of FF2 with dust elements in the afternoon (Fig. 10) may suggest the formation of SOA on existing dust particles, which would not be included in the ACSM OM as this component would be associated with non-refractory material or larger particles not efficiently transmitted through the ACSM inlet. This hypothesis is consistent with the relatively small increase in the OOA-1 fraction observed by ACSM in the afternoon ($7 \pm 19\%$ on average), though it is also possible that the majority of SOA production from local emissions happens downwind of the measurement site. The STXM-NEXAFS single-particle analysis (example images and spectra shown in Fig. 12) supports the hypothesis that some of the discrepancy in the FTIR and ACSM measurements of organic aerosol may be explained by the fraction of OM associated with non-refractory material; 33 out of 39 particles analyzed indicated organic aerosol mixed with dust

Please cite this article in press as: Takahama, S., et al., Submicron organic aerosol in Tijuana, Mexico, from local and Southern California sources during the CalMex campaign, Atmospheric Environment (2012), http://dx.doi.org/10.1016/j.atmosenv.2012.07.057

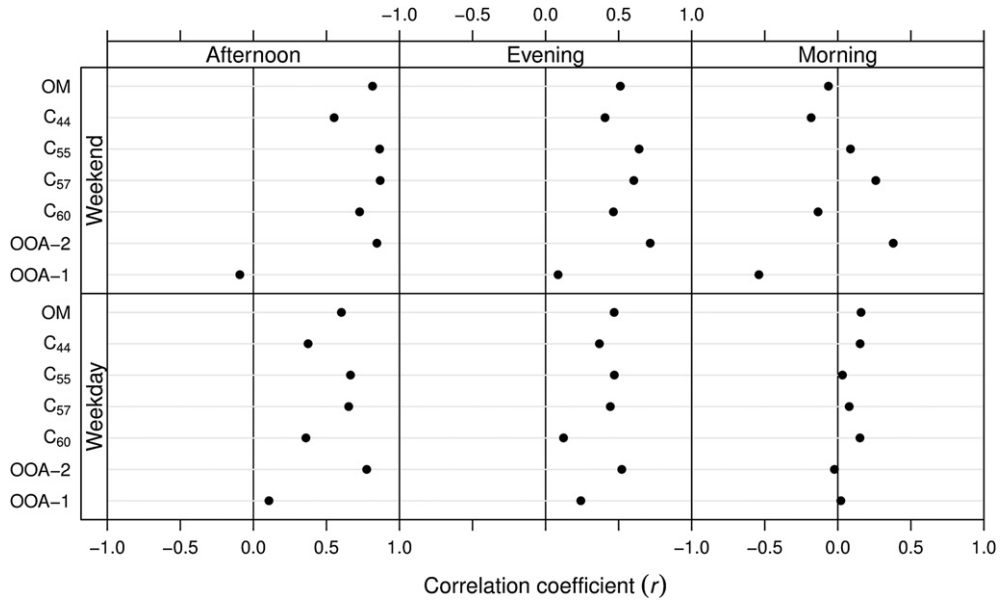

Fig. 13. Correlations of BC with ACSM OM, mass fragments, and PMF components. C_x is the OM-equivalent mass concentration of mass fragment (m/z) x.

($n = 15$; 1–3.5 μm) or BC ($n = 30$; 0.2–3.1 μm), and six carboxylic-acid dominated particles (Takahama et al., 2007) (1.4–4.6 μm). Additionally, the marine aerosol is not correlated with ACSM OM ($r = 0.10$), presumably because the OM is associated with non-refractory, larger sea salt particles.

3.3. Geographical origins of source contributions

HYSPLIT backtrajectories from Tijuana indicate that the airmass consistently originated from the west and northwest quadrant (Fig. 14) without much variation by time of day, week, or speed. These quadrants include San Diego, Tijuana, and the intermediate border region, which are likely origins of the less oxygenated OM that correlates in with BC and VOC emissions that are likely to be from automobiles. In previous studies, the more oxygenated fraction of OM has been apportioned to locally-produced SOA and background OM based on diurnal occurrence and correlation with VOC tracers (de Gouw et al., 2009; Liggio et al., 2010; Liu et al., 2011). A delayed correlation of OOA-1 with anthropogenic VOCs (Fig. S5; maximum $r = 0.26$ delayed by one or two hours) may suggest some production of SOA at the site; however, the increase in OOA-1 fraction of OM between morning and afternoon periods at this measurement site is on average 7 ± 19% (the actual OOA-1 and OM concentrations decrease, on average, but largely due to differences in boundary-layer heights). The relatively uniform O/C ratio and OOA-1 fractions suggest that a large fraction of OM (estimated as 60% for an upper bound from the OOA-1 fraction) is transported to Parque Morelos from more regional sources (and contains a mixture of sources, as described in Section S2.1). There are several possible explanations, which include advection of urban aerosol to the Pacific Ocean during the daytime and returning during the night due to land-sea breeze (LSB) circulation. This effect has been reported by Cass and coworkers (Shair et al., 1982; Cass and Shair, 1984) for the Los Angeles (LA) area, and this sub-grid-scale phenomenon is not captured by the HYSPLIT backtrajectories as the model calculates mean wind vectors derived from archived GDAS meteorology assimilated with a spatial resolution of 40 km. Despite the regularity in the temporal cycle of anthropogenic emissions, examination of the marine aerosol fraction of OM from PMF on FTIR measurements does not indicate a strong diurnal pattern, which would be expected to be low during the day and higher during the evening for a strong, local LSB influence. The marine aerosol fraction is highest during successive periods extending over several days, indicating the larger influence of synoptic-scale meteorology in regulating the marine fraction of aerosol. While Ault et al. (2009) and Hawkins and Russell (2010) report large contributions of LA aerosol to the mass budget of OM in San Diego, backtrajectories from Tijuana and forward trajectories from LA during this period indicate that the major path of advection from LA was not directed through San Diego and Tijuana during the CalMex campaign period. However, it is possible that the source of the oxygenated aerosol may be Southern California pollution advected to sea through LSB circulation and transported to this measurement site in Tijuana. LSB circulation may also explain the

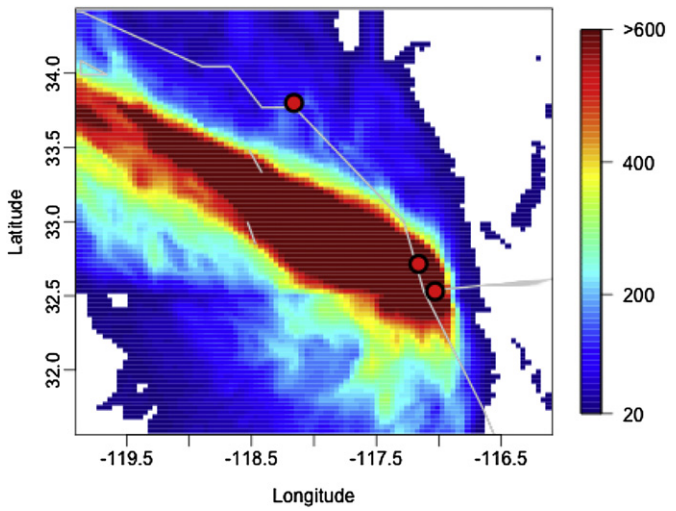

Fig. 14. Density image of backtrajectories from Tijuana for starting altitudes of 10, 100, and 500 m a.g.l. The color scale bounds values between 10th and 90th percentile of the hourly-trajectory points falling in a 40 km × 40 km grid in the displayed domain. The circles indicate the location of major cities, from north to south: LA, San Diego, and Tijuana. (For interpretation of the references to color in this figure legend, the reader is referred to the web version of this article.)

Please cite this article in press as: Takahama, S., et al., Submicron organic aerosol in Tijuana, Mexico, from local and Southern California sources during the CalMex campaign, Atmospheric Environment (2012), http://dx.doi.org/10.1016/j.atmosenv.2012.07.057

observed increases in concentrations of inorganic aerosol nitrate during the early morning periods (Fig. 2), which may be transported to the site following production of nitric acid through the N_2O_5 pathway in a humidified environment over the ocean. Entrainment of free-troposphere aerosol from above the shallow marine boundary layer (200–300 m on average during daytime) cannot be ruled out, but the source of pollution in FT is unlikely to be large and consistent enough to account for the OM measured. Transport from west of Los Angeles would require 10–24 h (for wind speeds of 2–5 m s^{-1} estimated from HYSPLIT calculations; Section S3); this interpretation is consistent with the observed O/C values indicative of urban outflow (Aiken et al., 2008), and lack of strong diurnal variations observed in the OOA-1 fraction during this campaign. This meteorological pattern is not likely to be an isolated phenomena observed only during this campaign; simulation and reanalysis over longer timescales (six years) suggest that north easterly winds due to the Pacific Subtropical High (PSH) system is a common meteorological pattern in the region (Zhao et al., 2011).

4. Conclusions

PM_1 organic aerosol composition was measured by FTIR, ACSM, and STXM-NEXAFS. Combining these measurements with statistical analysis methods (factor and classification analyses), additional measurements (e.g., BC, VOCs) and meteorological models, the OM mass was apportioned to various source classes and a dominant source region. Synthesizing organic aerosol measurements from various instruments, we can make several statements about the concentration, sources, and origins of OM in Tijuana. The campaign-average OM concentration was 3.3 ± 1.7 μg m^{-3} (approximately 53 ± 14% of NR-PM_1), with anthropogenic combustion, biomass burning, and marine sources contributing to this aerosol burden. The aerosol was very oxygenated according to ACSM analysis, with average O/C ratios of 0.64 ± 0.19. The PMF and classification analyses suggest that the more oxygenated fraction of the OM is likely to be aged OM transported to Tijuana rather than locally-produced SOA. A large contribution of oxygenated aerosol from various source classes was inferred; some fraction of oxygenated (secondary) organic aerosol may be associated with non-refractory components, such as dust or BC. Backtrajectory simulations using the HYSPLIT model suggest that the mean wind vector consistently originated from the northwest region, over the Pacific Ocean. Much of the aged aerosol (as much as 60% of the OM and containing a mixture of sources, based on quantification of the highly oxygenated fraction) is likely to have been transported to Tijuana from pollution advected to sea by a sub-grid scale land-sea breeze circulation off the coast of Southern California. Anthropogenic combustion is estimated to contribute approximately 40–60% to the OM mass at Parque Morelos, and 40–50% of this is likely to be due to local sources, such as automobile traffic. The marine aerosol contribution to OM during the period was on average 23 ± 24%, though its contribution varied over synoptic rather than diurnal timescales. OM from BB aerosol contributed 20 ± 20% and the OM during the campaign period, with notable BB events occurring during several weekend evenings. OM observed during this period were less oxygenated (apportioned to the OOA-2 factor) and different in composition from previously reported BBOA (according to magnitudes of the estimated f_{60} metric), consistent with their co-occurrence with elements normally associated with industrial or anthropogenic emissions (S, V). The more oxygenated component of anthropogenically-derived OM reported by FTIR PMF analysis appears to be SOA formed on mineral dust surfaces, which was not captured by the ACSM (similarly with marine aerosol) as it was associated with non-refractory particles.

Acknowledgments

The authors would like to thank: the Molina Center and the participants of the CalMex campaign who assisted with logistics and sample collection (particularly Luisa T. Molina, Hugo Barrera, Miguel Zavala, Claudia Rivera, Aldo Cortez, and Bianca Puckita); Zhan Zhao for her expertise in meteorological analysis; Ashley Corrigan for helpful comments on the PMF analysis; John T. Jayne for ACSM operation in the field; and Phil Croteau and Sally Ng for assistance and software for preparation of measurement error matrix for PMF analysis of ACSM mass spectra. Funding for this work was provided by NSF AGS-1009408, with logistical costs supported by CARB 09-356. The statements and conclusions in this paper are those of the researchers (contractor) and not necessarily those of CARB. The mention of commercial products, their source, or their use in connection with material reported herein is not to be construed as actual or implied endorsement of such products.

Appendix A. Supplementary data

Supplementary data related to this article can be found at http://dx.doi.org/10.1016/j.atmosenv.2012.07.057.

References

Aiken, A.C., Decarlo, P.F., Kroll, J.H., Worsnop, D.R., Huffman, J.A., Docherty, K.S., Ulbrich, I.M., Mohr, C., Kimmel, J.R., Sueper, D., Sun, Y., Zhang, Q., Trimborn, A., Northway, M., Ziemann, P.J., Canagaratna, M.R., Onasch, T.B., Alfarra, M.R., Prevot, A.S.H., Dommen, J., Duplissy, J., Metzger, A., Baltensperger, U., Jimenez, J.L., 2008. O/C and OM/OC ratios of primary, secondary, and ambient organic aerosols with high-resolution time-of-flight aerosol mass spectrometry. Environmental Science & Technology 42 (12), 4478–4485.

Ault, A.P., Moore, M.J., Furutani, H., Prather, K.A., May 2009. Impact of emissions from the Los Angeles port region on San Diego air quality during regional transport events. Environmental Science & Technology 43 (10), 3500–3506.

Bahadur, R., Uplinger, T., Russell, L.M., Sive, B.C., Cliff, S.S., Millet, D.B., Goldstein, A., Bates, T.S., 2010. Phenol groups in northeastern us submicrometer aerosol particles produced from seawater sources. Environmental Science & Technology 44 (7), 2542–2548.

Border, 2012. US Mexico Environmental Program, Indicators Report, 2005. Tech. rep. http://www.epa.gov/usmexicoborder/docs/BorderIndicatorsReportApril2006.pdf.

Cass, G., Shair, F., 1984. Sulfate accumulation in a sea breeze/land breeze circulation system. Journal of Geophysical Research 89 (D1), 1429–1438. URL: http://www.agu.org/journals/ABS/1984/JD089iD01p01429.shtml.

Cubison, M.J., Ortega, A.M., Hayes, P.L., Farmer, D.K., Day, D., Lechner, M.J., Brune, W.H., Apel, E., Diskin, G.S., Fisher, J.A., Fuelberg, H.E., Hecobian, A., Knapp, D.J., Mikoviny, T., Riemer, D., Sachse, G.W., Sessions, W., Weber, R.J., Weinheimer, A.J., Wisthaler, A., Jimenez, J.L., 2011. Effects of aging on organic aerosol from open biomass burning smoke in aircraft and laboratory studies. Atmospheric Chemistry and Physics 11 (23), 12049–12064. URL: http://www.atmos-chem-phys.net/11/12049/2011/.

Day, D.A., Liu, S., Russell, L.M., Ziemann, P.J., 2010. Organonitrate group concentrations in submicron particles with high nitrate and organic fractions in coastal southern California. Atmospheric Environment 44 (16), 1970–1979.

de Gouw, J.A., Welsh-Bon, D., Warneke, C., Kuster, W.C., Alexander, L., Baker, A.K., Beyersdorf, A.J., Blake, D.R., Canagaratna, M., Celada, A.T., Huey, L.G., Junkermann, W., Onasch, T.B., Salcido, A., Sjostedt, S.J., Sullivan, A.P., Tanner, D.J., Vargas, O., Weber, R.J., Worsnop, D.R., Yu, X.Y., Zaveri, R., 2009. Emission and chemistry of organic carbon in the gas and aerosol phase at a sub-urban site near Mexico city in march 2006 during the Milagro study. Atmospheric Chemistry and Physics 9 (10), 3425–3442.

Dockery, D.W., Pope, C.A., Xu, X.P., Spengler, J.D., Ware, J.H., Fay, M.E., Ferris, B.G., Speizer, F.E., Dec. 1993. An association between air-pollution and mortality in 6 United-States cities. New England Journal of Medicine 329 (24), 1753–1759.

Draxler, R., Rolph, G., 2010. Hysplit (Hybrid Single-particle Lagrangian Integrated Trajectory) Model Access via NOAA Arl Ready Website. http://ready.arl.noaa.gov/hysplit.php.

Fine, P.M., Cass, G.R., Simoneit, B.R.T., Apr. 2002. Chemical characterization of fine particle emissions from the fireplace combustion of woods grown in the southern United States. Environmental Science & Technology 36 (7), 1442–1451.

Fortner, E.C., Zheng, J., Zhang, R., Knighton, W.B., Volkamer, R.M., Sheehy, P., Molina, L., Andre, M., 2009. Measurements of volatile organic compounds using proton transfer reaction – mass spectrometry during the Milagro 2006 campaign. Atmospheric Chemistry and Physics 9 (2), 467–481.

Frossard, A.A., Shaw, P.M., Russell, L.M., Kroll, J.H., Canagaratna, M.R., Worsnop, D.R., Quinn, P.K., Bates, T.S., 2011. Springtime arctic haze contributions of submicron organic particles from European and Asian combustion sources. Journal of Geophysical Research-atmospheres 116.

Garnes, L.A., Allen, D.T., Oct. 2002. Size distributions of organonitrates in ambient aerosol collected in Houston, Texas. Aerosol Science and Technology 36 (10), 983–992.

Ge, X., Wexler, A.S., Clegg, S.L., Jan. 2011. Atmospheric amines – part i. A review. Atmospheric Environment 45 (3), 524–546.

Hamilton, J.F., Webb, P.J., Lewis, A.C., Hopkins, J.R., Smith, S., Davy, P., Aug. 2004. Partially oxidised organic components in urban aerosol using GCXGC-TOF/MS. Atmospheric Chemistry and Physics 4, 1279–1290.

Hawkins, L.N., Russell, L.M., 2010. Oxidation of ketone groups in transported biomass burning aerosol from the 2008 northern California lightning series fires. Atmospheric Environment 44 (34), 4142–4154.

Hennigan, C.J., Sullivan, A.P., Collett, Jeffrey, L.J., Robinson, A.L., May 2010. Levoglucosan stability in biomass burning particles exposed to hydroxyl radicals. Geophysical Research Letters 37, L09806.

Henry, R.C., 2003. Multivariate receptor modeling by n-dimensional edge detection. Chemometrics and Intelligent Laboratory Systems 65 (2), 179–189.

Jayne, J.T., Leard, D.C., Zhang, X.F., Davidovits, P., Smith, K.A., Kolb, C.E., Worsnop, D.R., 2000. Development of an Aerosol Mass Spectrometer for size and composition analysis of submicron particles. Aerosol Science and Technology 33 (1–2), 49–70.

Jimenez, J.L., Canagaratna, M.R., Donahue, N.M., Prevot, A.S.H., Zhang, Q., Kroll, J.H., DeCarlo, P.F., Allan, J.D., Coe, H., Ng, N.L., Aiken, A.C., Docherty, K.S., Ulbrich, I.M., Grieshop, A.P., Robinson, A.L., Duplissy, J., Smith, J.D., Wilson, K.R., Lanz, V.A., Hueglin, C., Sun, Y.L., Tian, J., Laaksonen, A., Raatikainen, T., Rautiainen, J., Vaattovaara, P., Ehn, M., Kulmala, M., Tomlinson, J.M., Collins, D.R., Cubison, M.J., Dunlea, E.J., Huffman, J.A., Onasch, T.B., Alfarra, M.R., Williams, P.I., Bower, K., Kondo, Y., Schneider, J., Drewnick, F., Borrmann, S., Weimer, S., Demerjian, K., Salcedo, D., Cottrell, L., Griffin, R., Takami, A., Miyoshi, T., Hatakeyama, S., Shimono, A., Sun, J.Y., Zhang, Y.M., Dzepina, K., Kimmel, J.R., Sueper, D., Jayne, J.T., Herndon, S.C., Trimborn, A.M., Williams, L.R., Wood, E.C., Middlebrook, A.M., Kolb, C.E., Baltensperger, U., Worsnop, D.R., Dec. 2009. Evolution of organic aerosols in the atmosphere. Science 326 (5959), 1525–1529.

Jobson, B.T., Alexander, M.L., Maupin, G.D., Muntean, G.G., Aug. 2005. On-line analysis of organic compounds in diesel exhaust using a proton transfer reaction mass spectrometer (PTR-MS). International Journal of Mass Spectrometry 245 (1–3), 78–89.

Kanakidou, M., Seinfeld, J.H., Pandis, S.N., Barnes, I., Dentener, F.J., Facchini, M.C., Van Dingenen, R., Ervens, B., Nenes, A., Nielsen, C.J., Swietlicki, E., Putaud, J.P., Balkanski, Y., Fuzzi, S., Horth, J., Moortgat, G.K., Winterhalter, R., Myhre, C.E.L., Tsigaridis, K., Vignati, E., Stephanou, E.G., Wilson, J., 2005. Organic aerosol and global climate modelling: a review. Atmospheric Chemistry and Physics 5, 1053–1123.

Laskin, A., Smith, J.S., Laskin, J., May 2009. Molecular characterization of nitrogen-containing organic compounds in biomass burning aerosols using high-resolution mass spectrometry. Environmental Science & Technology 43 (10), 3764–3771.

Liggio, J., Li, S.-M., Vlasenko, A., Sjostedt, S., Chang, R., Shantz, N., Abbatt, J., Slowik, J.G., Bottenheim, J.W., Brickell, P.C., Stroud, C., Leaitch, W.R., Nov. 2010. Primary and secondary organic aerosols in urban air masses intercepted at a rural site. Journal of Geophysical Research-atmospheres 115, D21305.

Lindinger, W., Hansel, A., Jordan, A., Sep. 1998. Proton-transfer-reaction mass spectrometry (PTR-MS): on-line monitoring of volatile organic compounds at PPTV levels. Chemical Society Reviews 27 (5), 347–354.

Liu, S., Day, D.A., Shields, J.E., Russell, L.M., 2011. Ozone-driven daytime formation of secondary organic aerosol containing carboxylic acid groups and alkane groups. Atmospheric Chemistry and Physics 11 (16), 8321–8341. URL: http://www.atmos-chem-phys.net/11/8321/2011/.

Liu, S., Takahama, S., Russell, L.M., Gilardoni, S., Baumgardner, D., 2009. Oxygenated organic functional groups and their sources in single and submicron organic particles in Milagro 2006 campaign. Atmospheric Chemistry and Physics 9 (18), 6849–6863.

Ng, N.L., Canagaratna, M.R., Zhang, Q., Jimenez, J.L., Tian, J., Ulbrich, I.M., Kroll, J.H., Docherty, K.S., Chhabra, P.S., Bahreini, R., Murphy, S.M., Seinfeld, J.H., Hildebrandt, L., Donahue, N.M., DeCarlo, P.F., Lanz, V.A., Prevot, A.S.H., Dinar, E., Rudich, Y., Worsnop, D.R., 2010. Organic aerosol components observed in northern hemispheric datasets from aerosol mass spectrometry. Atmospheric Chemistry and Physics 10 (10), 4625–4641.

Ng, N.L., Canagaratna, M.R., Jimenez, J.L., Zhang, Q., Ulbrich, I.M., Worsnop, D.R., Feb. 2011a. Real-time methods for estimating organic component mass concentrations from Aerosol Mass Spectrometer data. Environmental Science & Technology 45 (3), 910–916.

Ng, N.L., Herndon, S.C., Trimborn, A., Canagaratna, M.R., Croteau, P.L., Onasch, T.B., Sueper, D., Worsnop, D.R., Zhang, Q., Sun, Y.L., Jayne, J.T., 2011b. An aerosol chemical speciation monitor (ACSM) for routine monitoring of the composition and mass concentrations of ambient aerosol. Aerosol Science and Technology 45 (7). pii: 934555189.

Paatero, P., Tapper, U., 1994. Positive matrix factorization – a nonnegative factor model with optimal utilization of error-estimates of data values. Environmetrics 5 (2), 111–126.

Russell, L.M., 2003. Aerosol organic-mass-to-organic-carbon ratio measurements. Environmental Science & Technology 37 (13), 2982–2987.

Russell, L.M., Bahadur, R., Ziemann, P.J., 2011. Identifying organic aerosol sources by comparing functional group composition in chamber and atmospheric particles. Proceedings of the National Academy of Sciences of the United States of America 108 (9), 3516–3521.

Russell, L.M., Hawkins, L.N., Frossard, A.A., Quinn, P.K., Bates, T.S., 2010. Carbohydrate-like composition of submicron atmospheric particles and their production from ocean bubble bursting. Proceedings of the National Academy of Sciences of the United States of America 107 (15), 6652–6657.

Russell, L.M., Takahama, S., Liu, S., Hawkins, L.N., Covert, D.S., Quinn, P.K., Bates, T.S., 2009. Oxygenated fraction and mass of organic aerosol from direct emission and atmospheric processing measured on the R/V Ronald Brown during TEXAQS/GoMACCS 2006. Journal of Geophysical Research-atmospheres 114.

Schwartz, R.E., Russell, L.M., Sjostedt, S.J., Vlasenko, A., Slowik, J.G., Abbatt, J.P.D., Macdonald, A.M., Li, S.M., Liggio, J., Toom-Sauntry, D., Leaitch, W.R., 2010. Biogenic oxidized organic functional groups in aerosol particles from a mountain forest site and their similarities to laboratory chamber products. Atmospheric Chemistry and Physics 10 (11), 5075–5088.

Schwarz, J.P., Spackman, J.R., Gao, R.S., Perring, A.E., Cross, E., Onasch, T.B., Ahern, A., Wrobel, W., Davidovits, P., Olfert, J., Dubey, M.K., Mazzoleni, C., Fahey, D.W., 2010. The detection efficiency of the single particle soot photometer. Aerosol Science and Technology 44 (8). pii: 924376370.

Seinfeld, J.H., Pandis, S.N., 2006. Atmospheric Chemistry and Physics, second ed. John Wiley & Sons, New York.

Shair, F., Sasaki, E., Carlan, D., Cass, G., Goodin, W., Edinger, J., Schacher, G., 1982. Transport and dispersion of airborne pollutants associated with the land breeze–sea breeze system. Atmospheric Environment (1967) 16 (9), 2043–2053. URL: http://linkinghub.elsevier.com/retrieve/pii/000469818290275X.

Stöhr, J., 1992. NEXAFS Spectroscopy. Springer-Verlag, Berlin.

Sullivan, A.P., Holden, A.S., Patterson, L.A., McMeeking, G.R., Kreidenweis, S.M., Malm, W.C., Hao, W.M., Wold, C.E., Collett, J.L., 2008. A method for smoke marker measurements and its potential application for determining the contribution of biomass burning from wildfires and prescribed fires to ambient PM2.5 organic carbon. Journal of Geophysical Research-atmospheres 113.

Takahama, S., Liu, S., Russell, L.M., 2010. Coatings and clusters of carboxylic acids in carbon-containing atmospheric particles from spectromicroscopy and their implications for cloud-nucleating and optical properties. Journal of Geophysical Research-atmospheres 115.

Takahama, S., Pathak, R.K., Pandis, S.N., Apr. 2007. Efflorescence transitions of ammonium sulfate particles coated with secondary organic aerosol. Environmental Science & Technology 41 (7), 2289–2295.

Takahama, S., Russell, L.M., Jan. 2011. A molecular dynamics study of water mass accommodation on condensed phase water coated by fatty acid monolayers. Journal of Geophysical Research-atmospheres 116, D02203.

Takahama, S., Schwartz, R.E., Russell, L.M., Macdonald, A.M., Sharma, S., Leaitch, W.R., 2011. Organic functional groups in aerosol particles from burning and non-burning forest emissions at a high-elevation mountain site. Atmospheric Chemistry and Physics 11 (13), 6367–6386.

Ulbrich, I., Lechner, M., Jimenez, J., 2012. AMS Spectral Database. URL: http://cires.colorado.edu/jimenez-group/AMSsd/.

Ulbrich, I.M., Canagaratna, M.R., Zhang, Q., Worsnop, D.R., Jimenez, J.L., 2009. Interpretation of organic components from positive matrix factorization of aerosol mass spectrometric data. Atmospheric Chemistry and Physics 9 (9), 2891–2918.

Warneke, C., De Gouw, J.A., Kuster, W.C., Goldan, P.D., Fall, R., Jun. 2003. Validation of atmospheric voc measurements by proton-transfer-reaction mass spectrometry using a gas-chromatographic preseparation method. Environmental Science & Technology 37 (11), 2494–2501.

Zhang, Q., Alfarra, M.R., Worsnop, D.R., Allan, J.D., Coe, H., Canagaratna, M.R., Jimenez, J.L., Jul. 2005. Deconvolution and quantification of hydrocarbon-like and oxygenated organic aerosols based on aerosol mass spectrometry. Environmental Science & Technology 39 (13), 4938–4952.

Zhang, Q., Jimenez, J.L., Canagaratna, M.R., Allan, J.D., Coe, H., Ulbrich, I., Alfarra, M.R., Takami, A., Middlebrook, A.M., Sun, Y.L., Dzepina, K., Dunlea, E., Docherty, K., DeCarlo, P.F., Salcedo, D., Onasch, T., Jayne, J.T., Miyoshi, T., Shimono, A., Hatakeyama, S., Takegawa, N., Kondo, Y., Schneider, J., Drewnick, F., Borrmann, S., Weimer, S., Demerjian, K., Williams, P., Bower, K., Bahreini, R., Cottrell, L., Griffin, R.J., Rautiainen, J., Sun, J.Y., Zhang, Y.M., Worsnop, D.R., Jul. 2007. Ubiquity and dominance of oxygenated species in organic aerosols in anthropogenically-influenced northern hemisphere midlatitudes. Geophysical Research Letters 34 (13), L13801.

Zhao, J., Zhang, R.Y., May 2004. Proton transfer reaction rate constants between hydronium ion ($H_3O^{(+)}$) and volatile organic compounds. Atmospheric Environment 38 (14), 2177–2185.

Zhao, J., Zhang, R.Y., Misawa, K., Shibuya, K., Dec. 2005. Experimental product study of the OH-initiated oxidation of m-xylene. Journal of Photochemistry and Photobiology A-chemistry 176 (1–3), 199–207.

Zhao, Z., Chen, S.-H., Kleeman, M.J., Tyree, M., Cayan, D., Jul. 2011. The impact of climate change on air quality-related meteorological conditions in California. Part i: present time simulation analysis. Journal of Climate 24 (13), 3344–3361.

Please cite this article in press as: Takahama, S., et al., Submicron organic aerosol in Tijuana, Mexico, from local and Southern California sources during the CalMex campaign, Atmospheric Environment (2012), http://dx.doi.org/10.1016/j.atmosenv.2012.07.057